ORIGINAL PAPER

Optimization of large capacity six-strand tundish with flow channel for adapting situation of fewer strands casting

Cheng Yao[1] · Min Wang[1] · Ming-xu Pan[2] · Yan-ping Bao[1]

Abstract

Closing a single nozzle or multiple nozzles for a temporary casting operation (fewer strands casting) was common in a tundish due to insufficient molten steel or equipment failure. However, nozzle clogging usually happens under the situation of fewer strands casting. Hence, a temperature deviation index was introduced to characterize the temperature stratification of molten steel for a large capacity tundish, and a new calculation method of residence time curve was used to describe the different flow types of molten steel at each outlet. Based on hydraulics experiment and numerical simulation, important parameters of present case and modified case were compared. Under the situation of fewer strands casting, the proportion of internal-recycle flow after modification decreased from 30.68% to 24.55%; the standard deviation of the response time reduced from 27.59 to 13.16, and the interquartile range of temperature deviation index changed from 0.89 to 0.27.

Keywords Large capacity tundish · Fewer strands casting · Internal-recycle flow · Strands consistency · Temperature deviation index

1 Introduction

With the development of metallurgical technology, the tundish played an effective and efficient role in homogenizing the composition and temperature of molten steel and removing nonmetallic inclusions from molten steel. A large capacity tundish could increase the residence time (RTD) of molten steel and reduce fluctuation of the steel-slag interface during the ladle change operation. It was more and more widely used in Chinese steel mills [1, 2]. In field production, problems such as insufficient supply of molten steel or equipment failure often occurred; hence, it was necessary to close a single nozzle or multiple nozzles for a temporary casting operation, which was usually referred to as fewer strands casting, to ensure the production rhythm and to ensure that continuous casting matched the refining cycle of ladle furnace (LF) and Ruhrstahl Heraeus (RH) refining furnace [3, 4]. The extreme complexity of the flow

field and temperature field in the situation of fewer strands casting made many phenomena worth being studied. In general, the large capacity tundish could make the molten steel flow state more complex, and it needed to be optimized by effective measures. On the one hand, it was important to install flow control devices such as turbulence inhibitor, weir and dam, or adopt new technologies such as electromagnetic stirring and argon blowing to improve the flow state of melt and the consistency of strands [5–10]. On the other hand, it was indispensable to find out specific and effective quantitative indicators to describe the flow characteristics of molten steel and to evaluate the quality of molten steel flow [11, 12].

According to the combined model theory, the volume of molten steel in a tundish was divided into plug-flow volume, well-mixed volume and dead zone volume. As a rule, the plug-flow volume was relevant with the removal performance of inclusions, and the dead zone volume was relevant with the effective flow volume of molten steel. Meanwhile, there was no qualitative explanation for the advantages and disadvantages of the well-mixed volume. The RTD curve was usually used to evaluate the flow characteristics in a tundish. Previous studies on the RTD curve mainly focused on the steady state flow in a multiple

✉ Min Wang
wangmin@ustb.edu.cn

1 State Key Laboratory of Advanced Metallurgy, University of Science and Technology Beijing, Beijing 100083, China

2 Daye Special Steel Co., Ltd., Huangshi 435000, Hubei, China

flow tundish, including consistency of strands or double peaks phenomena of the RTD curve [13–16]. RTD descriptions of the flow characteristics under the situation of fewer strands casting in a large capacity tundish were seldom reported because of the extremely complex flow characteristic and large well-mixed volume.

Temperature field was also a necessary index to characterize the flow state of molten steel [17, 18]. The large capacity tundish usually had multiple strands, and the large temperature difference of molten steel between multiple strands was a symbol of poor flow characteristics of molten steel. In addition, high temperature in the mold could easily cause centerline segregation or breakout accidents during continuous casting and low temperature in the mold could easily cause nozzle blockage. Under the situation of fewer strands casting, the temperature and energy exchange between newly added molten steel and residual molten steel in the tundish more easily resulted in the temperature stratification, which aggravated the temperature difference between strands. It was very important to get the detail temperature field during casting process.

This paper focused on a large capacity six-strand T-type tundish from a Chinese special steel plant and introduced the temperature deviation index to characterize the temperature stratification of molten steel; a new calculation method of RTD curve was used to describe the different flow types of molten steel at each outlet. Based on hydraulics experiment and numerical simulation, the important reference indexes of different cases were analyzed under the situation of fewer strands casting, and then, the restricted links of nozzle clogging were found. This research work can provide a basis for the operation of a large capacity tundish to adapt the situation of fewer strands casting.

2 Experiment description

2.1 Tundish description

A six-strand tundish with a nominal capacity of 66 t from a steel plant of China was chosen for experiments. The top view of the originally designed tundish is shown in Fig. 1a. The tundish was composed of three characteristic areas including impact area, casting area and two flow pipes. The flow pipes were originally used as an induction heating area; at present, the induction heating device was not installed. For the tundish to be used in time, the flow pipes were changed to a flow channel to contact with the impact area and the casting area. The top view of the present used tundish is shown in Fig. 1b. In the field production, problems such as insufficient molten steel supply or equipment failure often occur. It is necessary to adopt fewer strands

casting in the tundish to ensure the production rhythm and match the refining and smelting cycle of continuous casting with LF and RH furnace. Under the situation of fewer strands casting, although the control of superheat is reasonable, the rest working outlets may result in clogging, which could affect the production rhythm and even cause accidents. In this paper, a modified tundish, as shown in Fig. 1c, was designed, aiming to solve the above problems that the working outlets were easy to be clogged. The top width and bottom width of the flow channel changed from 1.2 and 0.9 m to 0.5 and 0.4 m, respectively; the V-type retaining wall changed to U-type retaining wall, and the slag retaining plate changed to slag retaining wall with pilot hole. The specific details are shown in Fig. 1, and the basic technological parameters of the tundish are shown in Table 1.

The various outlets of the six-strand symmetric tundish were defined as outlet 1, outlet 2, outlet 3, outlet 4, outlet 5 and outlet 6 from left to right. The study contained six cases; case 1, case 2 or case 3 were to simulate the fewer strands casting by closing the outlet 1, outlet 2 or outlet 3, respectively, under the present used tundish, and case 4, case 5 or case 6 were to simulate the fewer strands casting by closing the outlet 1, outlet 2 or outlet 3, respectively, under the modified tundish.

2.2 Description of hydraulics experiment

2.2.1 Preparation and procedure of hydrodynamics experiments

Figure 2a shows the hydraulic model with a ratio of 1:3 to the prototype based on the similarity principles in this paper, and the Froude number and Weber number [19, 20] of the model should be equal to those of the prototype and the ratios of velocity. The flow rate and characteristic length between the hydraulic model and the prototype can be obtained by Eq. (1).

$$\frac{v_p^2}{L_p} = \frac{v_m^2}{L_m} \tag{1}$$

where v_p and v_m are the velocities of the prototype and the hydraulic model, respectively; and L_p and L_m are the characteristic lengths of the prototype and the hydraulic model, respectively.

The hydraulics experiment process can be described as four stages, as shown in Fig. 2b, and the numbers in square brackets in Fig. 2b indicate the following stages. The first stage (Stage 1) was the process of storing water and appeared from flow time $t = 0$ to $t = t_r$ (t_r is time to regulate flow instruments), the second stage (Stage 2) was the process to regulate flow instruments and appeared from
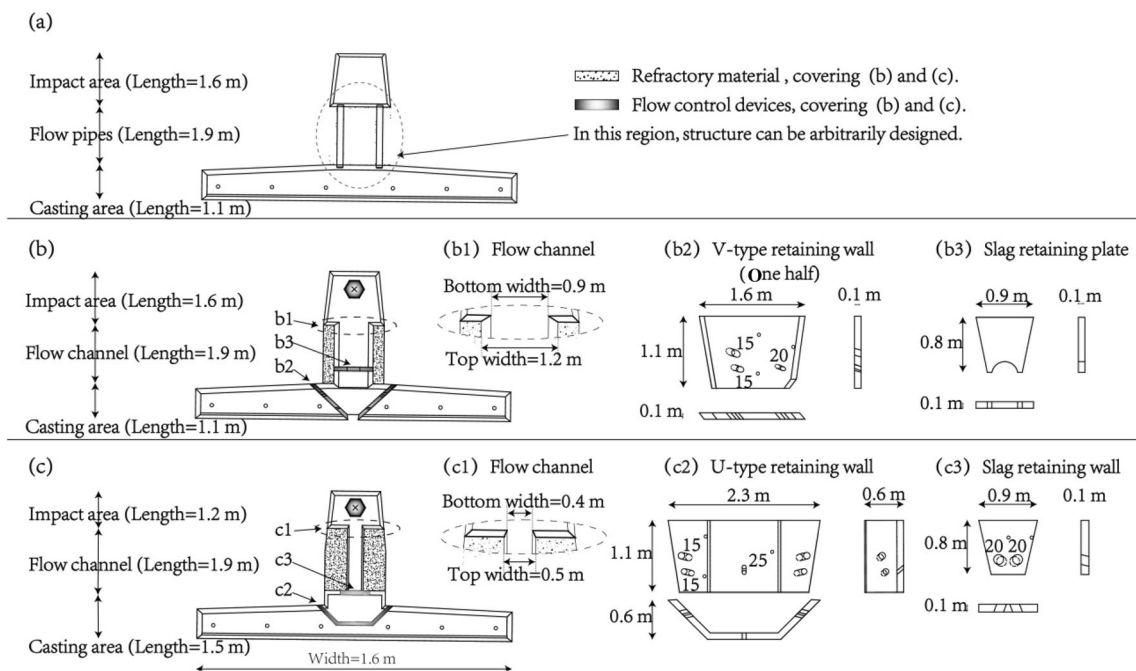
Fig. 1 Specific structure details of originally designed tundish (**a**), present used tundish (**b**) and modified tundish (**c**)

Table 1 Basic technological parameters of tundish

Casting condition	Unit	Value
Working capacity of ladle	t	120
Working capacity of tundish	t	60
Inner diameter of ladle shroud	mm	75
Outer diameter of ladle shroud	mm	130
Submergence depth of ladle shroud	mm	270
Height of molten steel	mm	900
Bloom cross section	mm × mm	320 × 390
Casting speed	m/min	0.6

$t = t_r$ to $t = t_0$ (t_0 is the tracer time), and the fourth state (Stage 4) was the process to drain away water and occurred after $t = 2.0t_s$ (t_s is the theoretical residence time). The third stage (Stage 3) was the experiment time to simulate the fewer strands casting and the "stimulation-response" method was used. When $t = t_0$, the liquid level in the tundish was stable at a specified height, 250 mL potassium chloride (KCl) was added by pulse from the tracer adding device on the ladle shroud, and the concentration information of the tracer was collected by conductance electrodes in outlets. From $t = t_0$ to $t = 2.0t_s$, the concentration information collected by the conductance electrodes was transmitted to the data acquisition system and the RTD curve was automatically drawn by the data analysis system. Figure 2c shows the details of the RTD curve and three

typical types of curves at the peak, including that (1) there was only one wave peak, and the curve at the peak was smooth; (2) there were many wave peaks, and the values of each wave peak were close; and (3) there were many wave peaks, and there was a larger wave peak; and the position of the wave peak in different situations had been marked on Fig. 2c.

2.2.2 Description of traditional calculation method and new calculation method of RTD curve

The RTD curve was a common method to handle the collected information. In the traditional calculation method of RTD curve, the time of experiment measurement was 2.5 times the theoretical residence time of a tundish after the tracer adding. The characteristic volume of molten steel in the tundish was calculated by the characteristic time on RTD curve, including plug-flow volume, well-mixed volume and dead zone volume. The volume fraction of these three volumes in a tundish can be obtained by Eqs. (2)–(6):

$$t_s = \frac{V}{Q} \tag{2}$$

$$t_a = \int_0^\infty tc(t)\mathrm{d}t \bigg/ \int_0^\infty c(t)\mathrm{d}t \tag{3}$$

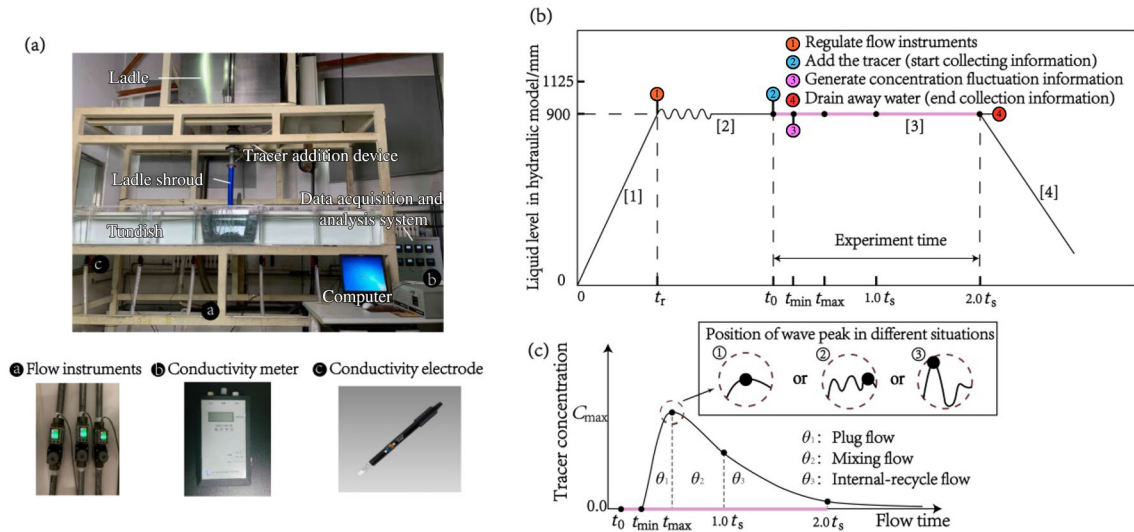$$\theta_d = 1 - \frac{t_a}{t_s} \tag{4}$$

Fig. 2 Hydraulics model (**a**), hydraulics experiment process (**b**) and RTD curve obtained by new method (**c**). t_{min} Response time; t_{max} peak time; C_{max} peak concentration

$$\theta_p = \frac{t_{min} + t_{max}}{2t_s} \quad (5)$$

$$\theta_m = 1 - \theta_d - \theta_p \quad (6)$$

where t_a is practical residence time, respectively; $c(t)$ is the tracer concentration at time t; V is the the total volume of molten steel; Q is the flow rate of molten steel; and θ_d, θ_p and θ_m are the plug-flow volume, well-mixed volume and dead zone volume, respectively.

However, the traditional calculation method of RTD curve was not suitable for the situation of fewer strands casting in a large capacity tundish. Taking the present used tundish as an example, the specific analyses are as follows:

(1) The theoretical residence time of hydraulic experiment was 879 s obtained through Eq. (2), and 2.5 times the theoretical residence time of hydraulic experiment was 2198 s, which could convert into the actual production time, about 3806 s, through $t_m = \lambda^{\frac{1}{2}} t_p$, where λ is a similarity ratio of the model to the prototype, and t_m and t_p are the model and prototype time, respectively. The time of continuous casting one heat steel in the actual production was only about 2400 s and the long experiment time could lead to the unnecessary and uncertainty of the results of the hydrodynamics experiment.

(2) The calculated well-mixed volume proportion of each strand was about 60%, which cannot reflect the difference of strands, and there was no systematic description of the advantages and disadvantages of the well-mixed volume. The data about well-mixed volume are from the analysis in Sect. 3.1.

(3) In view of the problem of nozzle clogging of fewer strands casting, it was more effective and efficient to study the flow types of molten steel flow at each outlet than to study the characteristic volumes of molten steel in tundish.

In this paper, a new calculation method of RTD curve was put forward to calculate the fewer strands casting in a large capacity tundish. The difference and connection between the new method and the traditional method are shown in Fig. 3b. In a nutshell, the traditional method was to calculate the characteristic volume of molten steel in a tundish and the new method was to calculate the flow types of molten steel flow at each outlet. The types of molten steel flowing out of the plug-flow volume were short-circuiting flow and plug flow. The types of molten steel flowing out of the well-mixed volume were mixing flow and internal-recycle flow. The measurement time of hydraulic experiment changed from 2.5 times the theoretical residence time to 2.0 times. In this paper, the internal-recycle flow is the molten steel flowing from the outlets between the 1.0 time the theoretical residence time and the 2.0 times the theoretical residence time.

In the meantime, Fig. 3a shows the flow field in 70 s of the hydraulic experiment and the result indicates that the guide hole on the V-type retaining wall in the experimental tundish had a good effect on the acceleration and guidance of the molten steel. Figure 3c shows the general trajectory of different flow types and the result indicates that after the tracer entering the casting area from the guide hole, the kinetic energy was sufficient, the tracer mainly concentrated in the upper area of outlet 4, and the short-circuiting flow can be basically eliminated, which means that the short-circuiting flow can be ignored by using the new
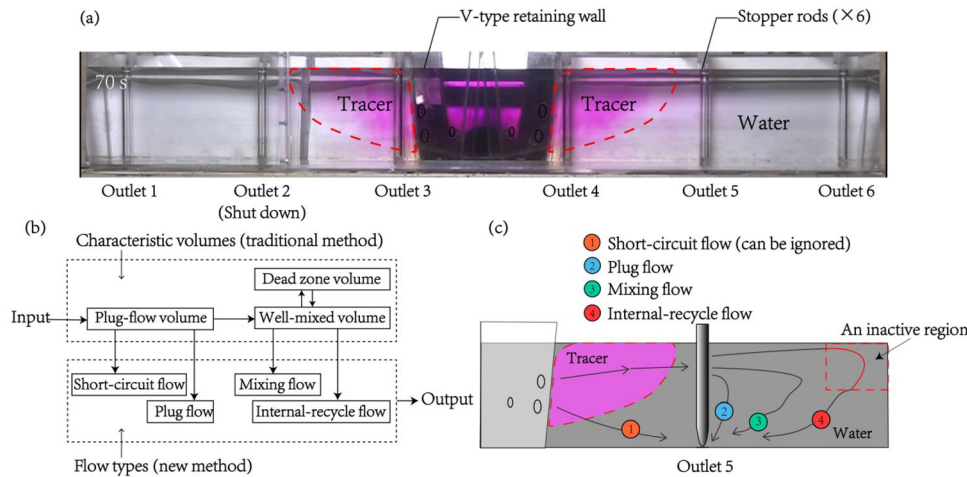
Fig. 3 Difference and connection between two methods (**a**), flow field in 70 s of hydraulic experiment (**b**) and flow types under new method (**c**)

method under the experimental tundish. The description of the new method is shown in Fig. 2c, where θ_1, θ_2 and θ_3 can be obtained by Eqs. (7)–(9).

$$\theta_1 = \int_{t_{\min}}^{t_{\max}} tc(t)\mathrm{d}t \Big/ \int_{t_{\min}}^{2t_s} tc(t)\mathrm{d}t \tag{7}$$

$$\theta_2 = \int_{t_{\max}}^{t_s} tc(t)\mathrm{d}t \Big/ \int_{t_{\min}}^{2t_s} tc(t)\mathrm{d}t \tag{8}$$

$$\theta_3 = \int_{t_s}^{2t_s} tc(t)\mathrm{d}t \Big/ \int_{t_{\min}}^{2t_s} tc(t)\mathrm{d}t \tag{9}$$

2.3 Description of numerical simulation

2.3.1 Basic assumptions

The molten steel flow in the tundish was a very complex turbulent flow and this paper made some basic assumptions in the calculation of numerical simulation.

(1) The molten steel flow in the tundish was treated as steady state flow, and the molten steel was considered as Newtonian and incompressible.

(2) The molten steel level was special shear wall boundary, ignoring the fluctuation of steel-slag interface and change of molten steel height.

(3) The effect of temperature on the density of the molten steel was ignored, and the density of the molten steel was constant.

(4) The physicochemical reaction between molten steel was ignored because the temperature and composition of molten steel entering the tundish previously and later were close.

2.3.2 Mathematical models

The equations that describe the transport of the turbulent energy k and dissipation rate ε could be expressed as follows:

$$\rho u_i \frac{\partial k}{\partial x_i} = \frac{\partial}{\partial x_i}\left(\frac{\mu_{\mathrm{eff}}}{\sigma_k} \times \frac{\partial k}{\partial x_i}\right) + G - \rho\varepsilon \tag{10}$$

$$\rho u_j \frac{\partial \varepsilon}{\partial x_j} = \left(\frac{\mu_{\mathrm{eff}}}{\sigma_\varepsilon} \times \frac{\partial \varepsilon}{\partial x_j}\right) + \frac{C_1 \varepsilon G}{k} - \frac{C_2 \rho \varepsilon^2}{k} \tag{11}$$

where $G = \mu_t \frac{\partial u_i}{\partial x_j}\left(\frac{\partial u_i}{\partial x_j} + \frac{\partial u_j}{\partial x_i}\right)$; ρ is the density of liquid steel, kg m^{-3}; x_i and x_j are the coordinates in the i and j direction; u is the velocity, m s^{-1}; subscripts i and j represent the coordinate directions; μ_{eff} is the effective viscosity, Pa s; $\mu_{\mathrm{eff}} = \mu_1 + \mu_t$; $\mu_t = \rho C_\mu \frac{k^2}{\varepsilon}$; μ_1 is the laminar viscosity, Pa s; μ_t is the turbulent viscosity, Pa s; and $C_1 = 1.43$, $C_2 = 1.93$, $C_\mu = 0.09$, $\sigma_k = 1.0$, and $\sigma_\varepsilon = 1.3$ are the empirical constants of the turbulence model.

Heat transfer model could be expressed as follows:

$$\frac{\partial\left(\rho C_p T u_i\right)}{\partial x_i} = \frac{\partial}{\partial x_i}\left(k_{\mathrm{eff}} \frac{\partial T}{\partial x_i}\right) \tag{12}$$

where k_{eff} is the effective thermal conductivity, $k_{\mathrm{eff}} = k_0 \frac{C_p \mu_i}{Pr_t}$, W/(m K); k_0 is the initial thermal conductivity, W/(m K); μ_i is the viscosity, kg/(m s); C_p is the specific heat capacity of liquid steel, J/(kg K); Pr_t is the turbulent Prandtl number; and T is the temperature, K.

Tracer diffusion model could be expressed as follows:

$$\frac{\partial(\rho C)}{\partial t} + \frac{\partial(\rho u_i C)}{\partial x_i} = \frac{\partial}{\partial x_i}\left(\rho D_{\mathrm{eff}} \frac{\partial C}{\partial x_i}\right) \tag{13}$$

where C is the tracer unquantifiable concentration; D_{eff} is the effective diffusivity, $D_{\mathrm{eff}} = D_m + D_t = D_m + \frac{D_{\mathrm{eff}}}{\rho Sc_t}$,

$m^2 \ s^{-1}$; D_m and D_t are the molecular and turbulent diffusivity, respectively, $m^2 \ s^{-1}$; and Sc_t is the turbulent Schmidt number.

2.3.3 Boundary conditions

According to the actual flow of fluid in a tundish, this paper set some boundary conditions in the calculation of numerical simulation.

(1) The inlet adopted the velocity-inlet condition, and the velocity direction was downward. The turbulent kinetic energy and the turbulent energy dissipation rate were calculated by $k = 0.01 v_{inlet}^2$ and $\varepsilon = {2k^{1.5}}/{D_{inlet}}$, where v_{inlet} is the inlet velocity, m/s, and D_{inlet} is the inner diameter of ladle shroud, m.

(2) The outlet also adopted the velocity-inlet condition, the velocity direction was downward, and the total flow rate of the outlet was equal to the flow rate of the inlet.

(3) The upper liquid level was set as the free surface and the shear force was set as zero.

(4) The solid wall surface of the tundish was non-slip wall surface, the standard wall function was used near the wall surface, and the gradient in normal direction was zero.

Numerical model parameters are shown in Table 2.

Table 2 Numerical model parameters

Numerical model parameter	Unit	Value
Density of liquid steel	kg/m³	6980
Viscosity of liquid steel	kg/(m s)	0.00614
Specific heat capacity of liquid steel	J/(kg K)	830
Thermal conductivity of liquid steel	W/(m K)	34.39
Inlet velocity	m/s	1.41245
Turbulence kinetic energy of inlet	m²/s²	0.02872
Dissipation rate of turbulence kinetic energy of inlet	m²/s³	0.12984
Inlet temperature	K	1820
Heat flux from free surface	W/m²	15,000
Heat flux from short side wall	W/m²	3800
Heat flux from long side wall	W/m²	3200
Heat flux from bottom	W/m²	1400
Gravitational acceleration	m/s²	9.81

2.3.4 Numerical method

In this paper, the tundish was divided into two symmetrical parts; one part of the grid was mirrored by another part of the divided grid at first, and then, the interface between the two parts was set as interior in computational fluid dynamics (CFD) software ANYSY-ICEM. Local grid encryption technology was used for ladle shroud and nozzles, and the grid in the calculation domain contained about 1,500,000 cells of non-uniform grid. Then, the control equation was solved by the CFD software ANYSY-Fluent, and the SIMPIEC algorithm was used for coupling the pressure and velocity terms. The convergence criterion was established when the sum of all residuals for the dependent variable was less than 10^{-4}. After the flow field was obtained for the steady state, the tracer diffusion model was solved for the unsteady state to obtain the RTD curve. Starting at $t = 0$ s, the model was run for ~ 3045 s using a constant time step of 0.01 s. Figure 4 shows the details of the numerical simulation process.

3 Results and discussion

3.1 Model validation and comparison of two calculation methods of RTD curve

In this paper, the hydraulic experiment and numerical simulation of fluid flow in a tundish were carried out by RTD curve, which was a common and useful tool to verify the similarity of the results. Taking case 2 as an example, the RTD curves of hydraulic experiment and numerical simulation were drawn, respectively, and then, the consistency of the two methods was verified by comparing the results of outlet 1 and outlet 4, as shown in Fig. 5. Outlet 1 and outlet 4 had the biggest difference in RTD curve characteristics. It was difficult to characterize the differences in RTD curve characteristics among all outlets together; thus, other outlets were deliberately ignored. The average residence time of outlet can be calculated by Eq. (3). The average residence time of outlet 1 in hydraulic experiment and numerical simulation was $1.03t_s$ and $0.98t_s$, respectively, and the average residence time of outlet 4 in hydraulic experiment and numerical simulation was $0.89t_s$ and $0.86t_s$, respectively, and the error of the numerical model was less than 5%. It indicates that the results of hydraulic experiment and numerical simulation were correct and reliable, and the results can be used in the study of the experimental tundish. Therefore, at the subsequent stage, the present used tundish and the modified tundish would be analyzed and studied by combining the two models.
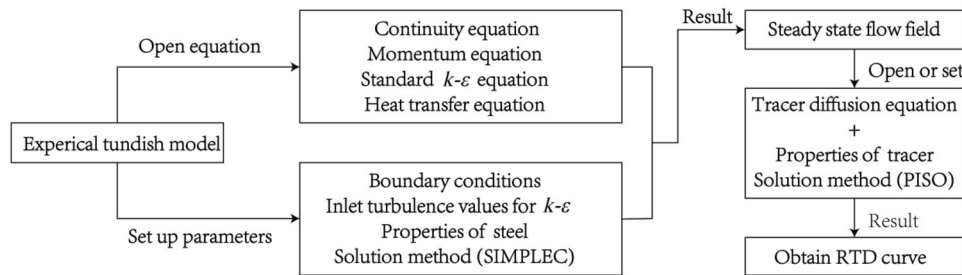
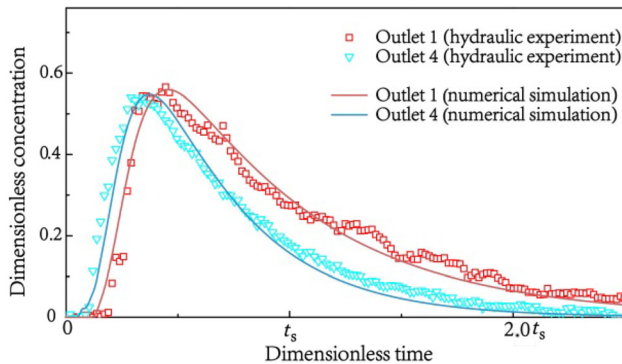Fig. 4 Details of numerical simulation process

Fig. 5 Verification of hydraulic experiment and numerical simulation

Table 3 shows the characteristic index of the flow field by using traditional method or new method. Under the situation of fewer strands casting, the side of the two working outlets was defined on the left side, and the side of the three working outlets was defined on the right side. Well-mixed volume in the traditional model and the internal-recycle flow in the new model were the two reference indexes most closely related to long residence time. Figure 6a shows the differences of the characteristic index in different cases, and the results show that the maximum difference in the well-mixed volume between different cases calculated by the traditional method was only 6.8%, which indicates that the traditional method did not compare the different modes of fewer strands casting in the same tundish structure and did not explain the difference of the left side and the right side in the same case. After using the new method, the maximum difference of the internal-recycle flow between different cases was 13.6%, and the difference between the characteristic of the left side and the right side in the same case can also be explained. The results show that the value by using new method can significantly show changes in the characteristic index between different cases. Figure 6b shows the differences in the characteristic index of different outlets, and the results show that the maximum difference in the internal-recycle flow between different outlets calculated by the new method was 14.3%, which indicates that the new method

can effectively and efficiently judge the differences between different outlets in same case.

3.2 Comparison of important flow indicators between different cases

The proportion of internal-recycle flow, as shown in Fig. 7, was taken as an index to represent the severity of internal circulation. Under the situation of fewer strands casting in the different tundishes, the proportion of internal-recycle flow reduced from the present average of 30.68% to the modified average of 24.55%, and the differences of internal-recycle flow reduced from the present average of 14.76% to the modified average of 5.9%. The results show that the internal circulation phenomenon was significantly improved in the modified tundish, and the residence time of molten steel was more reasonable, which could significantly reduce the potential for nozzle clogging.

In addition, the standard deviation (S) of the response time t_{min} of each strand, which was used as the evaluation standard for the consistency of strands, can be obtained by Eq. (14),

$$S = \sqrt{\sum_i^n (a_i - \bar{a})^2 / (n - 1)} \tag{14}$$

where a_i can be the tracer response time of the single strand RTD curve of the tundish; and $\bar{a}$ is the arithmetic mean value of the variable.

Under the situation of fewer strands casting in the different tundishes, the standard deviation decreased by more than half from the present average of 27.59 to the modified average of 13.16; the consistency of strands was obviously improved; and the molten steel can be timely and evenly distributed to each outlet after it entered the casting area, which ensured the effective replacement of newly added molten steel and residual molten steel.

Comparison of the response time between six cases is shown in Fig. 8. In case 2 or case 3, the difference of response time was about 71 s, and it illustrated that newly added molten steel took priority into the nearest working

Table 3 Characteristic index of flow field by using traditional method or new method (%)

Case	Characteristic index	Outlet 1	Outlet 2	Outlet 3	Outlet 4	Outlet 5	Outlet 6
Case 1	Plug-flow volume	–	19.9	17.2	15.7	16.9	18.4
	Well-mixed volume	–	67.4	67.4	66.8	62.9	70.2
	Dead zone volume	–	12.6	15.3	17.5	20.2	11.4
	Plug flow	–	12.5	19.0	23.5	23.1	28.1
	Mixing flow	–	53.9	49.2	49.1	51.4	38.2
	Internal-recycle flow	–	33.6	31.8	27.4	25.5	33.7
Case 2	Plug-flow volume	30.4	–	20.0	19.2	17.4	23.0
	Well-mixed volume	62.9	–	65.3	60.6	60.5	64.6
	Dead zone volume	6.6	–	14.6	20.1	22.1	12.4
	Plug flow	21.5	–	32.3	31.3	31.3	22.0
	Mixing flow	43.7	–	36.2	44.3	44.4	46.9
	Internal-recycle flow	34.7	–	31.5	24.5	24.2	31.1
Case 3	Plug-flow volume	36.2	28.6	–	25.7	24.1	29.8
	Well-mixed volume	62.3	63.1	–	62.5	63.1	63.5
	Dead zone volume	1.4	8.3	–	11.9	12.8	6.7
	Plug flow	21.0	23.3	–	28.5	26.3	14.9
	Mixing flow	40.0	43.1	–	43.6	46.3	50.8
	Internal-recycle flow	39.0	33.6	–	28.0	27.4	34.3
Case 4	Plug-flow volume	–	17.9	20.3	26.6	20.4	23.5
	Well-mixed volume	–	64.9	65.7	64.6	62.6	64.3
	Dead zone volume	–	17.2	14.1	8.8	17.0	12.2
	Plug flow	–	15.9	16.7	24.9	20.2	20.4
	Mixing flow	–	61.9	60.1	47.8	58.3	55.2
	Internal-recycle flow	–	22.2	23.2	27.3	21.4	24.4
Case 5	Plug-flow volume	30.2	–	27.0	27.1	22.6	27.0
	Well-mixed volume	59.3	–	64.2	67.4	65.6	64.9
	Dead zone volume	10.5	–	8.8	5.5	11.8	8.0
	Plug flow	26.1	–	21.4	18.5	17.2	19.4
	Mixing flow	49.0	–	53.4	53.4	59.0	54.7
	Internal-recycle flow	24.9	–	25.2	28.1	23.8	25.9
Case 6	Plug-flow volume	23.9	24.3	–	23.8	23.0	28.3
	Well-mixed volume	61.9	59.4	–	68.7	61.9	60.1
	Dead zone volume	14.2	16.3	–	7.5	15.0	11.6
	Plug flow	17.3	25.8	–	16.2	22.7	28.7
	Mixing flow	58.9	51.3	–	58.2	53.4	45.7
	Internal-recycle flow	23.8	22.9	–	25.7	24.0	25.6

outlet after entering the casting area and molten steel cannot be added to the rest outlets in time, which meant that there were large volume of fluid inactive areas near the furthest working outlet, with serious flow problems. Under the situation of fewer strands casting in the modified tundish, the difference of response time was about 31 s and the response time of outlets was shortened, which illustrated that the newly added molten steel can be distributed more evenly to the outlets and the flow field was optimized.

3.3 Comparison of temperature field between different cases

The temperature field was an important index to characterize the quality of molten steel during fewer strands casting. The uneven temperature distribution in the tundish could cause many harm, for example, (1) it could aggravate the instability of the growth thickness of the billet shell in the mold; (2) it could not be conducive to the floating
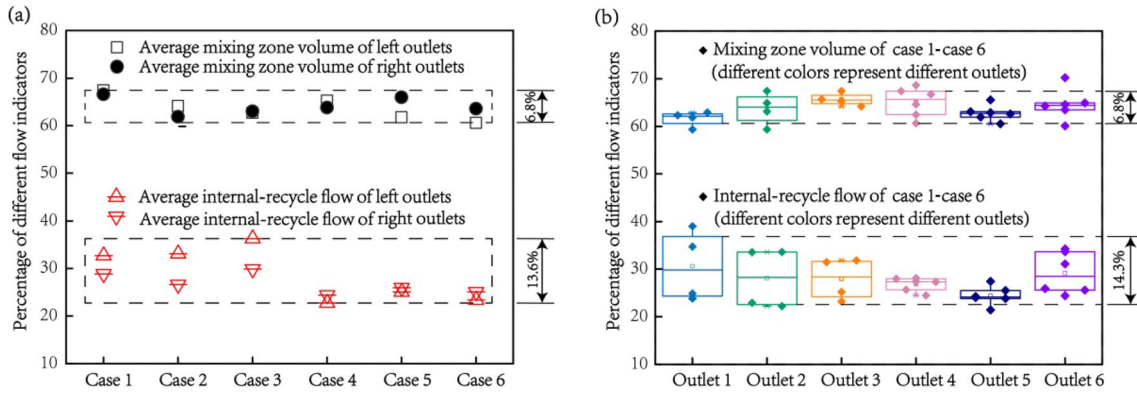
Fig. 6 Differences in characteristic index of different cases (**a**) and different outlets (**b**)
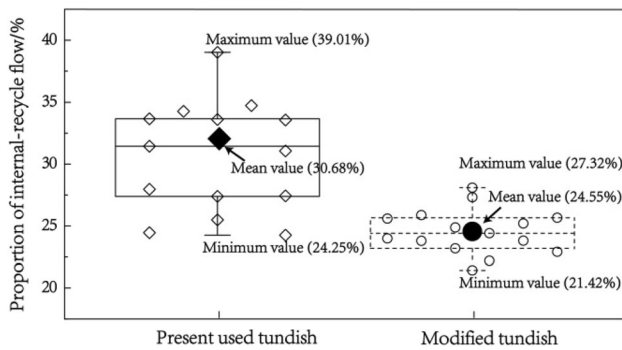

Fig. 7 Proportion of internal-recycle flow under present used tundish and modified tundish
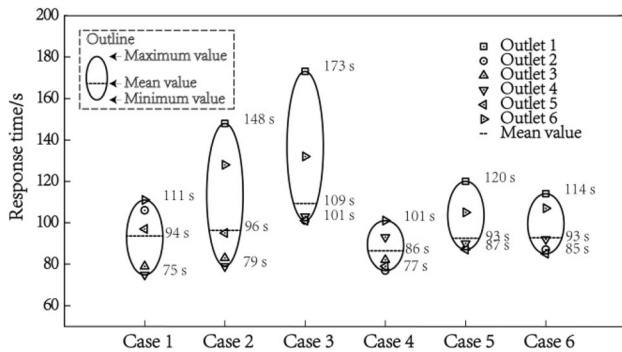

Fig. 8 Comparison of response time between six cases

removal of nonmetallic inclusions; and (3) it could produce the low-temperature molten steel region, and the low-temperature molten steel entering the outlet could lead to nozzle blocking.

The temperature field results at the longitudinal section of the outlets of different cases are shown in Fig. 9a. The results indicates that the temperature fields of case 1, case 2 and case 3 had same characters, while the temperature fields of case 4, case 5 and case 6 had same characters. In case 1, case 2 and case 3, the present used V-shaped retaining wall divided the casting area into two

independent sides. The temperature distribution on two sides was obviously non-uniform. The average temperature on the left side was lower than that on the right side, and the maximum temperature difference between the outlets was 5.0 K. By contrast, in case 4, case 5 and case 6, the modified U-shaped retaining wall could make the casting area connected as a whole and the molten steel can be added to most regions of the left side in time. The non-uniformity of the temperature distribution of the casting area was obviously optimized. The temperature distributions on the left side and the right side were similar, and the maximum temperature difference between the outlets was reduced by half from 5.0 K to a value below 2.5 K.

In order to quantitatively compare the temperature stratification of the regions around stopper rods in different cases, a new index, temperature deviation index, were proposed, which can be calculated by Eq. (15),

$$KT_i = \frac{T_1 - T_i}{T_1 - T_0} \tag{15}$$

where KT_i is the temperature deviation index; T_i is the temperature value at any temperature point of the section, K; T_0 is the average temperature at each point, K; and T_1 is the inlet temperature, K.

Figure 9b shows the boxplot elements and formulas, and Fig. 9c shows the relevant information of temperature deviation index in different cases. The interquartile range (IQR), which is the difference between the upper quartile (Q1) and the lower quartile (Q2), reflects the dispersion degree of the data in the middle 50% of each case. m in Fig. 9b represents the number of items of temperature point of the section. The low value of IQR indicates that the intermediate data were concentrated and the temperature stratification was not obvious. After using the modified tundish, IQR decreased from present average of 0.89 to modified average of 0.27, which illustrated that the temperature stratification phenomenon was significantly improved and the temperature distribution was more reasonable.
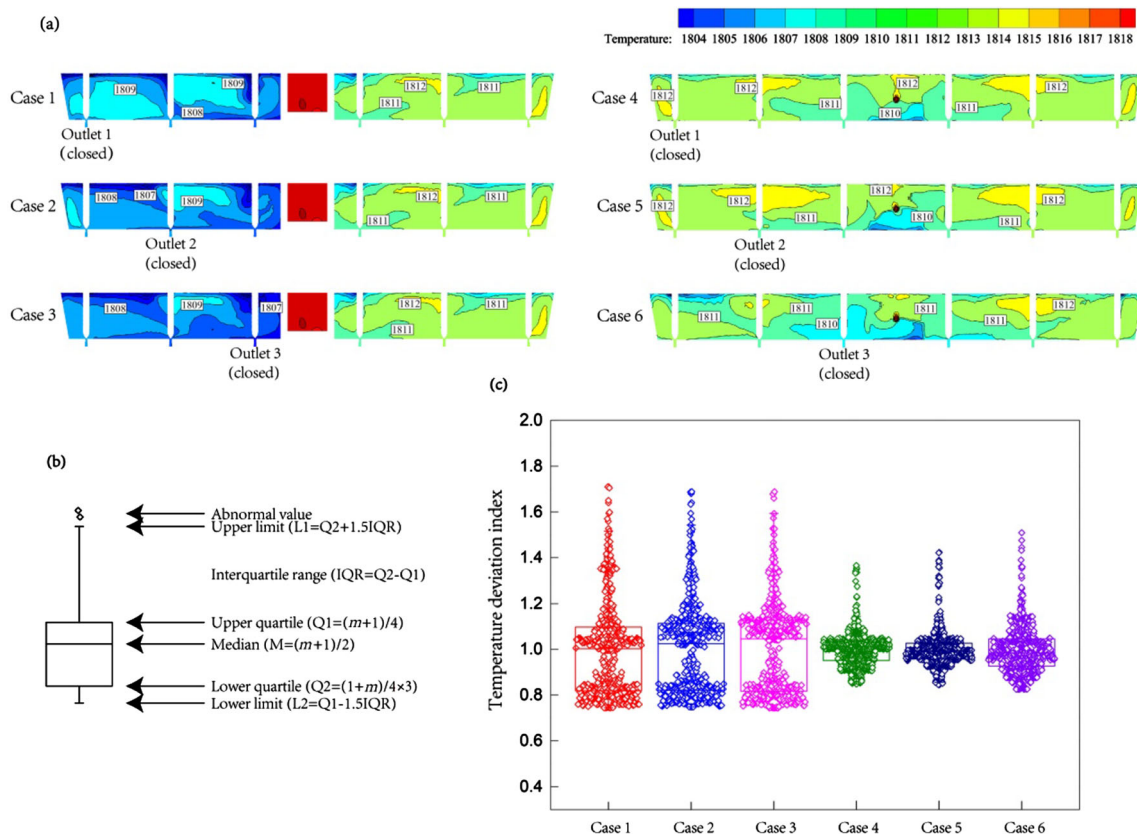
Fig. 9 Temperature field results of outlet longitudinal section of different cases (**a**), boxplot elements and formulas (**b**) and relevant information of temperature deviation index in different cases (**c**)

The flow field index and temperature field index were mutually verified. The results showed that due to the irrationality of present used tundish structure and flow control device, after the molten steel entering the casting area, the molten steel cannot reach the outlets evenly and the consistency of strands was also poor. At the same time, molten steel cannot supplement many regions of the left side (only two working outlets) in time. The flow velocity in these regions, accompanying serious internal circulation, was very slow. For a long time, these regions could easily become cold steel regions, where low-temperature molten steel accumulated, and then, the low-temperature molten steel entered into the working outlets, causing nozzle clogging. Compared with the present used tundish structure and flow control device, the modified tundish and flow control device were more reasonable, and each reference index was obviously optimized, which illustrates that using the modified tundish can effectively improve the consistency of strands, improve the temperature stratification phenomenon and prevent the occurrence of nozzle clogging.

4 Conclusions

1. A new calculation method of RTD curve is proposed. The value of the characteristic index by using the new calculation method could increase about twice compared to that of traditional method, which illustrated that the new method can significantly show variation between different cases or different outlets.

2. The standard deviation of the response time reduced from the present average of 27.59 to the modified average of 13.16. Maximum temperature difference of each outlet changed from the present average of 5.0 K to the modified average of 2.5 K. The consistency of strands, internal circulation phenomenon and temperature stratification was significantly improved.

3. Because of the irrationality of the present used tundish structure, the consistency of strands was poor, and the molten steel cannot be added to many regions on the left side (only two working outlets) of the casting area in time. The velocity in these regions, accompanying serious internal circulation, was very slow, which

could cause these regions to easily become cold steel regions, where low-temperature molten steel accumulated, and then the low-temperature molten steel entering into the working outlets could cause nozzle clogging.

4. The modified tundish structure was more reasonable and reference indexes were obviously optimized, which can provide a basis for the operation of a large capacity tundish to adapt the situation of fewer strands casting.

References

[1] S.G. Zheng, M.Y. Zhu, Y.L. Zhou, W. Su, J. Iron Steel Res. Int. 23 (2016) 92–97.

[2] J. Li, G.H. Wen, P. Tang, M.M. Zhu, Ironmak. Steelmak. 39 (2012) 140–146.

3 X.W. Huang, Continuous Casting 43 (2018) No. 3, 35–40.

[4] W.X. Xie, Y.P. Bao, L.Q. Zhang, M. Wang, R. Li, Foundry Technology 35 (2014) 2070–2072.

[5] N. Ding, Y.P. Bao, Q.S. Sun, L.F. Wang, Int. J. Miner. Metall. Mater. 18 (2011) 292–296.

[6] B. Yang, H. Lei, Y. Zhao, G.C. Xing, H.W. Zhang, Metals 9 (2019) 855.

[7] J. Palafox-Ramos, J. de Barreto, S. López-Ramírez, R.D. Morales, Ironmak. Steelmak. 28 (2001) 101–109.

[8] F. Xing, S.G. Zheng, M.Y. Zhu, Steel Res. Int. 89 (2018) 1700542.

[9] Q. Wang, F. Wang, B. Wang, Z.Q. Liu, B.K. Li, J. Iron Steel Res. Int. 19 (2012) No. S2, 969–972.

[10] C.J. Zhang, Y.P. Bao, M. Wang, L.C. Zhang, Int. J. Miner. Metall. Mater. 24 (2017) 47–54.

[11] T. Merder, J. Pieprzyca, M. Saternus, Metalurgija 53 (2014) 155–158.

[12] V. Singh, S.K. Ajmani, A.R. Pal, S.K. Singh, M.B. Denys, Ironmak. Steelmak. 39 (2012) 171–179.

[13] S.N. Lekakh, D.G.C. Robertson, ISIJ Int. 53 (2013) 622–628.

[14] Y.F. Wang, L.F. Zhang, ISIJ Int. 50 (2010) 1777–1782.

[15] S. Singh, S.C. Koria, ISIJ Int. 33 (1993) 1228–1237.

[16] G.C. Wang, M.F. Yun, C.M. Zhang, G.D. Xiao, ISIJ Int. 55 (2015) 984–992.

[17] J.B. Xie, J.A. Zhou, L.H. Zhou, B. Wang, H. Zhang, J. Iron Steel Res. Int. 24 (2017) 501–507.

[18] S. Sonoda, N. Murata, H. Hino, H. Kitada, M. Kano, ISIJ Int. 52 (2012) 1086–1091.

[19] M. Warzecha, T. Merder, H. Pfeifer, J. Pieprzyca, Steel Res. Int. 81 (2010) 987–993.

[20] C. Koria, S. Singh, ISIJ Int. 34 (1994) 784–793.